Gene clusters encoding putative outer membrane electron conduits have specific roles during metal and electrode respiration in *Geobacter sulfurreducens*.

Fernanda Jiménez Otero[a,b], Daniel R. Bond[a,b,c]

BioTechnology Institute[a], Department of Biochemistry, Molecular Biology, and Biophysics[b], Department of Plant and Microbial Biology[c] University of Minnesota-Twin Cities, Saint Paul MN 55108

Short title: Electron transfer across the outer membrane of *G. sulfurreducens*

Send all correspondence to:

Daniel R. Bond
140 Gortner Laboratory
1479 Gortner Ave
St. Paul, MN 55108
dbond@umn.edu

Keywords: *Geobacter*, extracellular electron transfer, multiheme cytochrome, porin cytochrome conduit

SUMMARY

At least five gene clusters in the *Geobacter sulfurreducens* genome encode putative outer membrane 'electron conduits', which are redox active complexes containing a periplasmic multiheme *c*-cytochrome, integral outer membrane β-barrel, and outer membrane redox lipoprotein. Single gene-cluster deletions and all possible multiple deletion mutant combinations were constructed and grown with graphite electrodes poised at +0.24 V and -0.1 V vs. SHE, Fe(III)- and Mn(IV)-oxides, and soluble Fe(III)-citrate. Different gene clusters were necessary for reduction of each electron acceptor. For example, only the Δ*extABCD* cluster mutant had a severe growth defect on graphite electrodes at all redox potentials, but this mutation did not affect Fe(III)-oxide, Mn(IV)-oxide, or Fe(III)-citrate reduction. During metal oxide reduction, deletion of the previously described *omcBC* cluster caused defects, but deletion of additional components in the Δ*omcBC* background, such as *extEFG,* was necessary to produce defects greater than 50% compared to wild type. Deletion of all five gene clusters was required to abolish all metal reduction. Mutants containing only one cluster were able to reduce particular terminal electron acceptors better than wild type, suggesting routes for improvement by targeting substrate-specific electron transfer pathways. Our results show *G. sulfurreducens* utilizes different membrane conduits depending on the extracellular acceptor used.

INTRODUCTION

Microorganisms capable of extracellular respiration can alter the redox state of particulate metal oxides in soils and sediments, controlling their solubility and bioavailability (Tadanier *et al.*, 2005; N'Guessan *et al.*, 2008; Toner *et al.*, 2009; Williams *et al.*, 2011; Yelton *et al.*, 2013; Couture *et al.*, 2015). To respire extracellular metals, bacteria must transfer electrons from the cell interior to outer surface redox proteins, requiring unique mechanisms compared to growth with soluble electron acceptors. The requirement for surface exposed electron transfer proteins also presents opportunities for transformation of heavy metals, biological nanoparticle synthesis, and a new generation of microbially-powered electrochemical devices using bacteria grown on electrodes (Bond *et al.*, 2002; Bond and Lovley, 2003; Holmes *et al.*, 2004; Ren *et al.*, 2008; Logan and Rabaey, 2012; Schrader *et al.*, 2016; Schievano *et al.*, 2016).

An extracellular electron transfer strategy must overcome several biological and inorganic issues. In Gram negative cells, a conductive pathway capable of crossing the inner membrane, periplasm, and outer membrane must first be constructed (Gralnick and Newman, 2007; Shi *et al.*, 2016). Because metal oxides vary widely in chemistry, surface charge, redox state, and surface area, an additional diversity of proteins may be needed to link cell surfaces with different terminal minerals (Navrotsky *et al.*, 2008; Majzlan, 2013; Levar *et al.*, 2017). Many metal-reducing bacteria can also transfer electrons to extracellular electrodes (Bond and Lovley, 2003; Marsili *et al.*, 2010; Snider *et al.*, 2012; Robuschi *et al.*, 2013). Unlike metal oxide particles, electrodes represent an unlimited electron acceptor where cells directly in contact with the inorganic surface can support more distant daughter cells linked by a conductive network of redox proteins that relay electrons to cells at the electrode. These biological and chemical variables raise the possibility that different electron transfer proteins may be needed to access each different kind of extracellular mineral, surface, or environment.

A model organism widely studied for its ability to reduce a diversity of metals and electrodes is the δ-Proteobacterium *Geobacter sulfurreducens*, and recent work suggests this organism can adjust its electron transfer pathway depending on conditions. CbcL, a combination *c*- and *b*-type inner membrane cytochrome (Zacharoff *et al.*, 2016), is only required when extracellular metals and electrodes are below redox potentials of -0.1 V vs. SHE, while the inner membrane *c*-type cytochrome ImcH (Levar *et al.*, 2014), is essential when acceptors are at higher redox potentials

(Levar *et al.*, 2017). Beyond the outer membrane, the secreted cytochrome OmcZ is needed only during electrode growth, while the secreted cytochrome PgcA only enhances reduction of Fe(III)-oxides (Nevin *et al.*, 2009; Leang *et al.*, 2010; Tremblay *et al.*, 2011; Qian *et al.*, 2011; Smith *et al.*, 2014; Peng and Zhang, 2017). Separating the initial event of inner membrane proton motive force generation from the extracellular protein-mineral interaction lies the outer membrane, an insulating barrier which was recently found to also contain electron transfer proteins of surprising complexity (Richardson *et al.*, 2012; Liu *et al.*, 2014).

A mechanism for electron transfer across the outer membrane is through a porin-cytochrome electron conduit, consisting of an integral outer membrane β-barrel proposed to anchor a periplasmic multiheme cytochrome to an outer surface lipoprotein cytochrome. By linking heme cofactors through the membrane spanning complex, electron flow is permitted (Hartshorne *et al.*, 2009; Richardson *et al.*, 2012). The first electron conduit described was the ~210 kDa MtrCAB complex from *S. oneidensis*, which can catalyze electron transfer across membranes to extracellular substrates when purified and placed in lipid vesicles (Wang *et al.*, 2008; Coursolle and Gralnick, 2012; White *et al.*, 2013). The *mtrCAB* gene cluster is essential for reduction of all tested soluble metals, electron shuttles, metal oxides, and electrodes by *S. oneidensis* (Baron *et al.*, 2009; Coursolle *et al.*, 2010; Coursolle and Gralnick, 2012). Related porin-cytochrome complexes capped with an extracellular DMSO reductase allow *Shewanella* to reduce DMSO on the cell exterior, while similar conduits support electron uptake by Fe(II)-oxidizing *Rhodopseudomonas* TIE-1 cells (Gralnick *et al.*, 2006; Jiao and Newman, 2007).

In *G. sulfurreducens*, a gene cluster encoding the periplasmic cytochrome OmbA, putative ß-barrel OmaB, and lipoprotein cytochrome OmcB also forms a conduit functionally similar to MtrCAB, though the two complexes lack any sequence similarity (Liu *et al.*, 2014). This '*ombB-omaB-omcB'* gene cluster is duplicated immediately downstream in the *G. sulfurreducens* genome as the near-identical '*ombC-omaC-omcC'*, together forming the '*omcBC*' cluster. Antibiotic cassette insertions within *omcB,* as well as insertions deleting the entire '*ombB-omaB-omcB'* conduit decrease growth with Fe(III) as an electron acceptor, but the impact differs between reports and growth conditions (Leang *et al.*, 2003; Leang and Lovley, 2005; Liu *et al.*, 2015). This variability between studies could be due to polar effects from inserted cassettes,

partial complementation by duplicated components, or the presence of undiscovered alternative pathways that also catalyze electron transfer across the outer membrane.

Recently, genome-wide transposon data found that insertions in *omcB* or *omcC* had no effect on *G. sulfurreducens* growth with electrodes poised at -0.1 vs. SHE, a low potential chosen to mimic the redox potential of Fe(III)-oxides (Chan *et al.*, 2017). However, transposon insertions within an unstudied four-gene cluster with porin-cytochrome signatures caused significant defects during growth on -0.1 V electrodes (Chan *et al.*, 2017). Deletion of this cluster, named *extABCD*, severely affected growth on low-potential electrodes, while Δ*extABCD* mutants grew similar to wild type with Fe(III)-oxides. In contrast, deletion of both conduits contained in the *omcBC* cluster had little impact on low-potential electrode growth. These data suggested that the outer membrane pathway used for electron transfer could vary depending on environmental conditions, but also raised new questions; are different conduits required at higher redox potentials, during growth with mineral forms such as Mn(VI), or when metals become soluble?

At least five electron conduits may be encoded in the genome of *G. sulfurreducens*. Using new markerless deletion methods, this study constructed combinations of mutants lacking these gene clusters, to simultaneously compare growth using Fe(III)- and Mn(IV)-oxides, poised electrodes at two different redox potentials, and soluble Fe(III)-citrate as terminal electron acceptors. We found that only strains lacking *extABCD* showed a growth defect when electrodes were the electron acceptor, and this effect was similar at all redox potentials. A strain containing *extABCD* but lacking all other conduit clusters grew faster and to a higher final density on electrodes. Phenotypes were more complex during metal reduction. The largest defects were in Δ*omcBC* strains, but deletion of the newly identified cluster *extEFG* in the Δ*omcBC* background was needed to severely inhibit Fe(III)-reduction. Deletion of all five clusters was necessary to eliminate reduction of soluble and insoluble metals tested. Strains containing only a single cluster showed preferences for reduction of different metals, such as the *extEFG*- and *extHIJKL*-only strains performing better with Mn(IV)-oxides than Fe(III)-oxides. These data provide evidence that multiple conduit clusters in the *G. sulfurreducens* genome are functional and are utilized during electron transfer in a substrate-dependent manner.

RESULTS

Description of putative outer membrane electron conduits. At least five gene clusters can be identified in the *G. sulfurreducens* genome encoding putative porin-cytochrome electron conduits, based on three key elements; (1) a multiheme periplasmic *c*-type cytochrome, (2) an outer membrane ß-barrel protein, and (3) one or more outer membrane lipoproteins with redox cofactors (Fig. 1A). Two of these clusters correspond to the well-studied OmcB-based (*omb*B-*oma*B-*omc*B, GSU2739-2737) conduit and its near-identical duplicate OmcC-based cluster immediately downstream (*omb*C-*oma*C-o*mc*C, GSU2733-2731). For clarity, and due to the fact that *omaBC* and *ombBC* are identical, these are together referred to as the "*omcBC*" cluster.

The *ext* genes comprise three new clusters, named for their putative roles in extracellular electron transfer (Chan *et al.*, 2017). The *extABCD* (GSU2645-2642) cluster encodes ExtA, a periplasmic dodecaheme *c*-cytochrome, ExtB, an outer membrane β-barrel with 18 trans-membrane domains, and ExtCD, two outer membrane lipoprotein *c*-cytochromes with 5 and 12 heme binding sites, respectively. The second cluster, *extEFG* (GSU2726-2724), encodes ExtE, an outer membrane β-barrel with 21 trans-membrane domains, ExtF, an outer membrane lipoprotein pentaheme *c*-cytochrome, and ExtG, a periplasmic dodecaheme *c*-cytochrome. The final cluster, *extHIJKL* (GSU2940-2936) lacks an outer membrane *c*-cytochrome, but encodes ExtH, a rhodanese-family lipoprotein, ExtI, a 21 trans-membrane domain outer membrane β-barrel, ExtK, a periplasmic pentaheme *c*-cytochrome, and ExtJL, two small outer membrane lipoproteins.

A significant difference between *G. sulfurreducens* Ext clusters and the *S. oneidensis* Mtr conduits (Hartshorne *et al.*, 2009), is that the porin-cytochrome conduits in *S. oneidensis* are paralogs. The periplasmic MtrA and MtrD cytochromes share over 50% identity, are similar in size and heme content, and can cross complement (Coursolle and Gralnick, 2010). The lipoprotein outer surface cytochromes of *Shewanella* also demonstrate high sequence, functional, and structural conservation (Coursolle and Gralnick, 2010; Clarke *et al.*, 2011; Richardson *et al.*, 2012; Edwards *et al.*, 2012). In contrast, no component of the Ext or OmcBC complexes share any homology. For example, the predicted periplasmic *c*-cytochromes ExtA,

ExtG, ExtK, and OmaB vary in size from 25 to 72 kDa, contain 5 to 15 hemes, and share 18%-26% identity (Fig. 1B).

To test physiological roles of these loci, single cluster mutants were first constructed, comprising Δ*extABCD, ΔextEFG,* Δ*extHIJKL,* and Δ*omb*B-*oma*B-*omc*B-*orfS-omb*C-*oma*C-o*mc*C (abbreviated as the Δ*omcBC* cluster) mutants. As these mutant strains lack any antibiotic cassettes, they were used as backgrounds for further deletions. Multiple cluster deletion mutants leaving only one conduit cluster on the genome are referred to by their single remaining cluster, e.g. "*extABCD*$^{+}$*" = ΔextEFG* Δ*extHIJKL* Δ*omcB*C*,* while the mutant lacking the *extABCD, extEFG, extHIJKL*, *omcB*-based and *omcC*-based clusters is referred to as "Δ5". These strains were tested under six different extracellular growth conditions varying in solubility, chemical composition, and redox potential.

Mutants lacking *extABCD* are defective in electrode growth at all redox potentials, while mutants containing only *extABCD* outperform wild type. When grown with electrodes poised at high (0.24 V vs. SHE) or low (-0.1 V, (Chan *et al.*, 2017)) redox potentials, only Δ*extABCD* mutants showed a defect in rate and extent of growth. Mutants lacking the *omcBC* and *extEFG* clusters grew similar to wild type, while Δ*extHIJKL* demonstrated a lag before growing with a similar doubling time as wild type to nearly wild type final current density (Fig. 2A). In all experiments, Δ*extABCD* grew slower than a 20 h doubling time, or over 3-fold slower than wild type, and could only achieve 20% of wild type final current density, or 116 ± 33 μA/cm^2 vs. 557 ± 44 μA/cm^2 (n ≥ 5).

Mutants containing only one gene cluster (*extABCD*$^{+}$, *extEFG*$^{+}$, *extHIJKL*$^{+}$, *omcBC*$^{+}$) as well as a mutant lacking all gene clusters (Δ5) were then analyzed for growth on electrodes. The Δ5 mutant grew at the low rate and extent of growth as the Δ*extABCD* single mutant at both redox potentials, suggesting than none of the additional clusters were responsible for residual growth originally seen in Δ*extABCD*. In contrast, *extABCD*$^{+}$ grew faster than wild type (4.5 ± 0.2 h vs. 6.5 ± 0.3 h doubling time, n ≥ 9) and reached a final current density 40% higher than wild type (768 ± 52 μA/cm^2 vs. 557 ± 44μA/cm^2, n≥9). All other multiple-deletion strains containing only

one cluster grew as poorly as the Δ5 mutant, further indicating that under these conditions, *extEFG*, *extHIJKL,* and *omcBC* did not contribute to electron transfer to electrodes (Fig. 2B).

A 5-conduit deletion mutant expressing *extABCD* has a faster growth rate on electrodes than wild type. To further investigate the specific effect of *extABCD* on electrode growth, *extABCD* was provided on a vector in the Δ5 strain. The 3-gene *omcB* conduit cluster (*omb*B-*oma*B-*omc*B) was also placed in the Δ5 strain using the same vector, and both were compared to wild type cells containing the empty vector. While the plasmid is stable for multiple generations, routine vector maintenance requires growth with kanamycin, and kanamycin carry-over into biofilm electrode experiments is reported to have deleterious effects on electrode growth (Levar *et al.*, 2014; Chan *et al.*, 2015). Thus, we re-examined growth of the empty vector strain. When selective levels of kanamycin (200 $\mu g \cdot ml^{-1}$) were present in electrode reactors, colonization slowed and final current production decreased 74%. At levels resulting from carry-over during passage of cells into the electrode reactor (5 $\mu g \cdot ml^{-1}$) growth rate was not affected, but final current was decreased up to 30%, suggesting interference with biofilm thickness rather than respiration (Fig. 3A). All subsequent complementation was performed in the presence of 5 $\mu g \cdot ml^{-1}$ residual kanamycin and compared to these controls.

Expressing the *omcB* conduit cluster in the Δ5 strain failed to increase growth with electrodes as electron acceptors. These data were consistent with the lack of an effect seen in Δ*omcBC* deletions, as well as the poor growth of *omcBC*$^{+}$ mutants containing both the OmcB and OmcC clusters (Fig. 3B). However, when *extABCD* was expressed on the same vector in the Δ5 background, colonization was faster and cells reached a higher final current density compared to wild type (421 ± 89 $\mu A/cm^2$ vs. 297 ± 11 $\mu A/cm^2$, n=3) (Fig. 3B). This enhancement was similar to the positive effect observed in the *extABCD*$^{+}$ strain, and further supported the hypothesis that *extABCD* played a central role during electron transfer to electrodes (Fig. 2B).

Growth of intermediate two-conduit deletion mutants were unchanged from single-cluster strains (Fig. S1). Just as the mutant lacking *extABCD* produced the same phenotype as the Δ5 strain (Fig. 2), deletion of second clusters from the Δ*extABCD* strain produced similar results as Δ*extABCD,* and no other two-cluster combination of *omcBC*, *extEFG* or *extHIJKL* mutants

showed defects to suggest they were utilized or expressed during these electrode growth conditions.

Cells lacking single gene clusters have partial reduction defects with Fe(III)- and Mn(IV)-oxides. In contrast to the dominant effect of *extABCD* on electrode respiration, no single cluster deletion eliminated the majority of growth with particulate Fe(III)- or Mn(IV)-oxides. The most severe defect was observed in the Δ*omcBC* cluster mutant, which reduced 68% of Fe(III)-oxide compared to wild type (Fig. 4A). Minor defects were observed for Δ*extEFG* and Δ*extHIJKL*, while Δ*extACBD* reduced Fe(III)-oxide near wild-type levels. None of the single mutants displayed defects with Mn(IV)-oxides (Fig. 4C). These results suggested that multiple clusters were active during metal oxide reduction.

Any one gene cluster is sufficient for partial Fe(III)- or Mn(IV)-oxide reduction, while deletion of all 5 clusters eliminates electron transfer to these metal oxides. Unlike electrode respiration, deletion of the full suite of clusters eliminated all residual electron transfer to Fe(III)-and Mn(IV)-oxides (Fig. 4B and D). When multiple-deletion strains containing only one cluster were tested for Fe(III)-oxide reduction, results supported key roles for *omcBC* and *extEFG* in metal oxide reduction, and little involvement by *extABCD*. For example, Fe(III)-oxide reduction by *omcBC*$^{+}$ was nearly 80% of wild type, *extEFG*$^{+}$ was over 60%, but the *extABCD*$^{+}$ strain reduced less than 30% of wild type. The *omcBC*$^{+}$, *extEFG*$^{+}$, and *extHIJKL*$^{+}$ strains achieved about 80% of wild type Mn(IV)-reduction at 80 hours, but the *extABCD*$^{+}$ strain again displayed poor growth with Mn(IV)-oxide.

Only strains lacking both *omcBC* and *extEFG* had a significant defect in Fe(III)- and Mn(IV)-oxide reduction. Because Δ*omcBC* demonstrated the largest defect in Fe(III)-oxide reduction, additional deletions in this background were tested for Fe(III) and Mn(IV)-oxide reduction (Fig. 5). Fe(III)-oxide reduction by Δ*omcBC* Δ*extEFG* was less than 25% of wild type, while the Δ*omcBC* Δ*extACBD*, and Δ*omcBC* Δ*extHIJKL* strains still reduced Fe(III)-oxides similar to the Δ*omcBC* strain. The Δ*omcBC* Δ*extEFG* strain also had a severe Mn(IV)-oxide reduction defect. Unlike Fe(III)-oxide reduction, the Δ*omcBC* Δ*extABCD* and Δ*omcBC*

Δ*extHIJKL* strains had a modest Mn(IV) reduction defect, suggesting contributions of the *extABCD* and *extHIJKL* clusters in the presence of Mn(IV) compared to Fe(III).

The poor growth of the Δ*omcBC* Δ*extEFG* mutant on insoluble metals was surprising since this strain still contained *extHIJKL,* and the *extHIJKL*$^{+}$ strain reduced 50% of Fe(III)-oxide and 75% of Mn(IV)-oxide compared to wild type (Fig. 4B and D; Table 2). This suggests *extHIJKL* expression or function of its product could be negatively affecting the level or activity of other clusters.

Expression of single conduit clusters partially recovers Fe(III)- and Mn(IV)-oxide reduction. When compared to empty-vector controls with low (5 μg·ml^{-1}) levels of kanamycin carryover, complementation of the Δ5 strain with single *omcB (*as *ombB-omaB-omcB*) or *extABCD* clusters resulted in partial recovery (Fig. 6), consistent with the intermediate phenotypes displayed by mutants retaining single clusters on the genome. Expression of the *omcB* cluster reestablished Fe(III)-oxide reduction, although to a level less than that seen in the *omcBC*$^{+}$ strain containing the full duplicated cluster (Fig. 4B). Expressing *extABCD* from a plasmid restored Fe(III)-oxide reduction in the Δ5 strain near the low levels of the *extABCD*$^{+}$ strain. Reduction of Mn(IV)-oxides by *omcB* or *extABCD*-expressing strains was even lower.

Only strains lacking both *omcBC* and *extABCD* had a significant defect in Fe(III)-citrate reduction. As with Fe(III)- and Mn(IV)-oxides, deletion of single conduit clusters in *G. sulfurreducens* only had modest effects on Fe(III)-citrate reduction (Fig. 7A) and additional conduit cluster deletions were needed to severely impact growth (Fig. 7B and C). The single cluster deletion strains Δ*omcBC*, Δ*extEFG,* and Δ*extHIJKL* still reduced ~60% of soluble Fe(III). However, in contrast to Fe(III)-oxides, the Δ*extABCD* strain showed near wild-type reduction. The Δ5 strain lacking all *omcBC* and *ext* clusters failed to reduce Fe(III)-citrate (Fig. 7B). Also unlike Fe(III)-oxide reduction, strains with only *omcBC*$^{+}$ or *extABCD*$^{+}$ clusters had near wild-type Fe(III)-citrate reduction rate, while *extEFG*$^{+}$ and *extHIJKL*$^{+}$ reduced Fe(III)-citrate to just 20% of wild type.

Since the Δ*omcBC* Δ*extEFG* strain showed the largest defect in Fe(III)-oxide reduction, this strain was analyzed with Fe(III)-citrate as well. However, this double cluster deletion mutant showed little difference compared to the parent Δ*omcBC* strain (Fig. 7C). In contrast to Fe(III)-

oxides, where deletion of *extABCD* had little effect, Δ*omcBC* Δ*extABCD* was the only conduit deletion combination that severely affected growth with Fe(III)-citrate (Fig. 7C). Compared to growth of *extEFG*$^{+}$ and *extHIJKL*$^{+}$ (Fig. 7B), the Δ*omcBC* Δ*extABCD* mutant (containing both *extEFG* and *extHIJKL*) reduced Fe(III)-citrate to the same level (Fig. 7C). These data suggest that when both *extEFG* and *extHIJKL* remained in the genome in the Δ*omcBC* Δ*extABCD* mutant, their activity was not additive. Plasmids containing either *ombB-omaB-omcB* or *extABCD* restored Fe(III)-citrate reduction in a Δ5 strain to levels within 90% of the respective *omcBC*$^{+}$ and *extABCD*$^{+}$ strains (Fig. 7D).

Not shown in Fig 7 is metal reduction data for intermediate deletion mutants such as Δ*extEFG* Δ*extHIJKL*. Screens performed after such double mutants were constructed revealed no changes to phenotypes that deviated from wild type or their parent single-cluster deletions. Only the intermediate strains with phenotypes, such as Δ*omcBC* background strains, are shown in Fig 7.

Proposed role(s) for the Omc and Ext electron conduits. Table 2 summarizes all extracellular reduction phenotypes of single cluster deletions and deletions leaving only one conduit, adjusted to wild type performance. Many of the recently described *ext* gene clusters are necessary for wild-type metal reduction, yet few are sufficient. For example, *extEFG* and *extHIJKL* were necessary for Fe(III)-citrate reduction, as strains lacking these clusters only reduced ~65% of wild type levels. But when only *extEFG* or *extHIJKL* was present, they were not sufficient to reduce Fe(III)-citrate to more than 25% of wild type levels.

In contrast, the *omcBC* cluster or the *extABCD* cluster alone was sufficient for Fe(III)-citrate reduction, and the *extABCD* cluster alone was sufficient for electrode growth. These phenotypes could be due to electron acceptor preferences of each complex, or differential expression driven by each electron acceptor, but in either case, each gene cluster was linked to phenotypes only under specific conditions. Deletion of all five conduits resulted in complete elimination of metal reduction abilities, while activity remained when the Δ5 strain was grown using electrodes as terminal electron acceptor. This comparison shows each gene cluster can be functional, but

only under particular conditions, and provides evidence for additional undiscovered pathways enabling transmembrane electron transfer.

DISCUSSION

Sequencing of the *G. sulfurreducens* genome revealed an unprecedented number of electron transfer proteins, with twice as many genes dedicated to respiratory and redox reactions as organisms with similarly-sized genomes (Methé *et al.*, 2003). Out of 111 *c*-type cytochromes, 43 had no known homolog, and many were predicted to reside in the outer membrane. The large complement of outer membrane redox proteins in *G. sulfurreducens* became even more of an anomaly as the electron transfer strategy of metal-reducing *S. oneidensis* emerged, where only a single outer membrane conduit was used to reduce a multitude of substrates (Wang *et al.*, 2008; Baron *et al.*, 2009; Coursolle *et al.*, 2010; Coursolle and Gralnick, 2010).

Evidence that more than one *G. sulfurreducens* outer membrane pathway exists for reduction of extracellular substrates has accumulated since the discovery of OmcB (Leang *et al.*, 2003). Deletion of *omcB* impacted Fe(III)-reduction, but had little effect on U(IV) or Mn(IV)-oxide reduction (Shelobolina *et al.*, 2007; Aklujkar *et al.*, 2013). A Δ*omcB* suppressor strain evolved for improved Fe(III)-citrate growth still reduced Fe(III)-oxides poorly (Leang and Lovley, 2005). Strains lacking *omcB* grew similar to wild type with electrodes in four different studies, (Holmes *et al.*, 2006; Richter *et al.*, 2009; Nevin *et al.*, 2009; Peng and Zhang, 2017), and OmcB abundance was lowest on cells near the electrode (Stephen *et al.*, 2014). An insertional mutant lacking six secreted and outer membrane-associated cytochromes in addition to *omcB* still demonstrated some Fe(III)-oxide reduction (Ueki *et al.*, 2017). After replacing the entire *omcBC* region with an antibiotic cassette and also finding residual Fe(III)-reducing ability, Liu *et al.* (2015) speculated that other porin-cytochrome-like clusters in the genome might be active. Most recently, Tn-seq analysis of electrode-grown cells found little effect of *omcB* mutations, yet noted significant defects from insertions in cytochromes with porin-cytochrome features (Chan *et al.*, 2017). This evidence led us to study if alternative *ext*-family conduits are functional in *G. sulfurreducens* under different conditions.

The genetic analysis presented here confirms a role for these unstudied conduits in extracellular respiration. All mutants still containing at least one cluster retained at least partial activity

376 towards metals, and deletion of the *omcBC* region, plus all three *ext* clusters, finally was able to
377 eliminate metal reduction. This need to delete more than one conduit cluster helps explain prior
378 variability and rapid evolution of suppressors in Δ*omcB*-only mutants. In the case of electrodes
379 at both high and low potentials, only deletion of *extABCD* affected growth. Since residual
380 electron transfer to electrodes was still detected after deletion of all clusters, additional
381 mechanisms remain to be discovered. Overall, these data support the conclusion that for all
382 tested metal and electrode acceptors, more than one conduit is functional and capable of
383 participating in electron transfer. We found no pattern of specific gene clusters being required at
384 particular redox potentials, suggesting that periplasmic proteins act as a 'translator' to interface
385 the array of outer membrane complexes with the energy conserving inner membrane
386 cytochromes ImcH and CbcL.
387
388 More difficult to resolve is whether each putative conduit is designed for interaction with specific
389 extracellular substrates. The fact that single cluster mutants performed differently with each
390 substrate, along with evidence that *omcB* could not complement electrode growth while
391 *extABCD* could, supports the hypothesis of substrate specificity. Promoters more active in the
392 presence of Fe(III) vs. Mn(IV) could create some of these phenotypes, but differential
393 expression still suggests cells prefer to use each cluster under specific conditions. Some
394 complexes may preferentially interact with secreted extracellular proteins who carry electrons to
395 the final destination, and activity from a complex is masked in the absence of its partner protein.
396 While many extracellular proteins are known to be involved in electron transfer, such as OmcS,
397 OmcE, OmcZ, PgcA, and pili, a lack of secreted proteins encoded within *omcBC* or *ext* gene
398 clusters argues against co-evolution of dedicated partners. The availability of strains containing
399 only one gene cluster will enable easier purification, engineered changes in expression levels,
400 and protein-protein interaction studies to test these hypotheses.
401
402 The genetic context of *ext* genes may aid identification of similar clusters in genomes of other
403 organisms, and reveal clues to their intended function. None of the *ext* regions fits the *mtr* 3-
404 gene 'porin cytochrome' operon of one small (~40 kDa) periplasmic cytochrome, a β-barrel, and
405 one large (>90 kDa) lipoprotein cytochrome. For example, *extABCD* includes two small
406 lipoprotein cytochromes, *extEFG* is part of a hydrogenase-family transcriptional unit, and
407 *extHIJKL* contains a rhodanese-like lipoprotein instead of an extracellular cytochrome (Fig. 1).
408 The transcriptional unit beginning with *extEFG* includes a homolog of YedY-family periplasmic

protein repair systems described in *E. coli* (Gennaris *et al.*, 2015), followed by a NiFe hydrogenase similar to bidirectional Hox hydrogenases used to recycle reducing equivalents in Cyanobacteria (Appel *et al.*, 2000; Coppi, 2005; Qiu *et al.*, 2010). Rhodanase-like proteins related to ExtH typically are involved in sulfur metabolism (Ravot *et al.*, 2005; Aussignargues *et al.*, 2012; Prat *et al.*, 2012) and an outer surface rhodanese-like protein is linked to extracellular oxidation of metal sulfides by *Acidithiobacillus ferrooxidans* (Ramírez *et al.*, 2002). Future searches for electron conduit clusters should consider the possibility of non-cytochrome components, and be aware that conduits might be part of larger complexes that could draw electrons from pools other than periplasmic cytochromes.

Including genes from *ext* operons in searches of other genomes reveals an interesting pattern in putative conduit regions throughout Desulfuromonadales strains isolated from freshwater, saline, subsurface, and fuel cell environments (Fig. 8). In about 1/3 of cases, the entire cluster is conserved intact, such as *extABCD* in *G. anodireducens, G. soli,* and *G. pickeringii* (Fig. 8B). However, when differences exist, they are typically non-orthologous replacements of the outer surface lipoprotein, such as where *extABC* is followed by a new cytochrome in *G. metallireducens, Geoalkalibacter ferrihydriticus,* and *Desulfuromonas soudanensis.* Conservation of the periplasmic cytochrome coupled to replacement of the outer surface redox protein also occurs in the *omcB* and *extHIJKL* clusters (Fig 8A and D). For example, of 18 *extHIJKL* regions, 10 contain a different extracellular rhodanese-like protein upstream of *extIJKL*, each with less than 40% identity to *extH*. This remarkable variability in extracellular components, compared to conservation of periplasmic redox proteins, suggests constant lateral gene transfer and selection of domains exposed to electron acceptors and the outside environment.

The data presented here significantly expands the number of outer membrane redox proteins contributing to electron transfer in *G. sulfurreducens*, and highlights a key difference in the *Geobacter* electron transfer strategy compared to other model organisms. In general, the pattern of multiple proteins with seemingly overlapping or redundant roles is less like respiratory reductases, and more reminiscent of cellulolytic bacteria that produce numerous similar β-glucosidases in response to a constantly changing polysaccharide substrate (Wang *et al.*, 2008; Coursolle *et al.*, 2010; Nelson *et al.*, 2017). A need for multiple outer membrane strategies could be a response to the complexity of metal oxides during reduction; minerals rapidly diversify to

become multiphase assemblages of more crystalline phases, the cell:metal interface can become enriched in Fe(II), and organic materials can bind to alter the surface (Cutting *et al.*, 2009; Coker *et al.*, 2012; Eusterhues *et al.*, 2014). Expressing a complex array of electron transfer pathways makes cells competitive at all stages with all electron acceptors, allowing *Geobacter* to outgrow more specialized organisms during perturbations in the environment.

EXPERIMENTAL PROCEDURES

Growth conditions.

All experiments were performed with our laboratory strain of *Geobacter sulfurreducens* PCA freshly streaked single colonies from freezer stocks. Anaerobic NB media (0.38 g/L KCl, 0.2 g/L NH_4Cl, 0.069 g/L $NaH_2PO_4H_2O$, 0.04 g/L $CaCl_22H_2O$, 0.2 g/L $MgSO_47H_2O$, 1% v/v trace mineral mix, pH 6.8, buffered with 2 g/L $NaHCO_3$ and flushed with 20:80 N_2:CO_2 gas mix) with 20 mM acetate as electron donor, 40 mM fumarate as electron acceptor was used to grow liquid cultures from colony picks. For metal reduction assays, 20 mM acetate was added with either 55 mM Fe(III) citrate, ~20 mM birnessite (Mn(IV)-oxide), or ~70 mM Fe(III)-oxide freshly precipitated from $FeCl_2$ by addition of NaOH and incubation at pH 7 for 1 h before washing in DI water. All experiments were carried out at 30°C.

Deletion and complementation construction

Putative conduits were identified through a genomic search for gene clusters containing loci predicted to encode a β-barrel using PRED-TMBB (Bagos *et al.*, 2004), contiguous to periplasmic and extracellular multiheme *c*-cytochromes or other redox proteins. Localization was predicted by comparing PSORT (Yu *et al.*, 2010) and the presence/absence of lipid attachment sites (Juncker *et al.*, 2003). Constructs to delete each gene cluster were designed to recombine to leave the site marker-free and also non-polar when located in larger transcriptional units, with most primers and plasmids for the single deletions described in Chan *et al.*, 2017. When genes were part of a larger transcriptional unit or contained an upstream promoter, it was left intact. For example, in the case of the *omcBC* cluster the transcriptional regulator *orfR*

(GSU2741) was left intact, and in *extEFG* the promoter and untranslated region was left intact so as to not disrupt the downstream loci.

For deletion mutant construction, the suicide vector pK18*mobsacB* (Simon *et al.*, 1983) with ~750 bp flanking to the target region was used to induce homologous recombination as previously described (Chan *et al.*, 2015). Briefly, two rounds of homologous recombination were selected for. The first selection used kanamycin resistance to select for mutants with the plasmid inserted into either up or downstream regions, and the second selection used sucrose sensitivity to select for mutants that recombine the plasmid out of the chromosome, resulting in either wild type or complete deletion mutants. Deletion mutants were identified using a kanamycin sensitivity test and verified by PCR amplification targeting the region. Multiple PCR amplifications with primers in different regions were used to confirm full deletion of each gene cluster (Chan *et al.*, 2017 and Table S1).

During this work, we found that manipulations in the *omcBC* cluster, which contains large regions containing 100% identical sequences, frequently underwent recombination into unexpected hybrid mutants which could escape routine PCR verification. For example, when the *omaB* and *omaC* genes recombined, a large hybrid operon containing *omaB*-linked to *ombC-omc*C would result. Routine primer screening, especially targeting flanking regions, failed to detect the large product. Only via multiple internal primers (Chan *et al.*, 2017 and Table S1), as well as longer-read or single molecule sequencing, were we able to verify and isolate strains in which complete loss of the *omcBC* cluster occurred, and dispose of hybrid mutants. Whole-genome resequencing was also performed on strains containing only one cluster, such as the strain containing only *extABCD*, especially since this strain has an unexpected phenotype where it produced more current than wild type. Thorough verification by PCR and whole genome sequencing are recommended to confirm deletions of large and repetitive regions such as the *omcBC* cluster.

Mutants lacking a single gene region were used as parent strains to build additional mutations. In this manner, six double gene-cluster deletion mutants, four triple-cluster deletion mutants and one quintuple-cluster deletion mutant lacking up to nineteen genes were constructed (Fig. 1; Table 1). For complementation strains, putative conduits were amplified using primers listed in Table S1 and inserted into the *G. sulfurreducens* expression vector pRK2-Geo2 (Chan *et al.*,

2015), which contains a constitutive promoter P_{acpP}. The putative conduit *extABCD* was assembled into a single transcriptional unit to ensure expression.

Electrode reduction assays

Sterile three-electrode conical reactors containing 15 mL of NB with 40 mM acetate as electron donor and 50mM NaCl to equilibrate salt concentration were flushed with a mix of N_2-CO_2 gas (80:20, v/v) until the O_2 concentration reached less than 2 ppm. Liquid cultures were prepared by inoculating 1 ml liquid cultures from single colonies inside an anaerobic chamber. Once these cultures reached late exponential to stationary phase, they were used to inoculate 10 ml cultures with 10% v/v. Each reactor was then inoculated with 25% v/v from this liquid culture as it approached acceptor limitation, at an OD_{600} between 0.48 and 0.52. Working electrodes were set at either -0.1 V or +0.24 V vs SHE and average current density recorded every 12 seconds. Each liquid culture propagated from an individual colony pick served no more than two reactors, and at least three separate colonies were picked for all electrode reduction experiments for a final $n \geq 3$.

Metal reduction assays

NB medium with 20 mM acetate as electron donor and either 55 mM Fe(III)-citrate, ~70 mM Fe(III) oxide, or ~20 mM birnessite ($Mn(IV)O_2$) as electron acceptor was inoculated with a 0.1% inoculum of early stationary phase fumarate limited cultures. Time points were taken as necessary with anaerobic and sterile needles. These were diluted 1:10 into 0.5 N HCl for the Fe(III) samples and into 2 N HCl, 4mM $FeSO_4$ for Mn(IV) samples. Samples were diluted once more by 1:10 in the case of Fe(III) assays and by 1:5 in the case of Mn(IV) assays into 0.5 N HCl. Ferrozine^R reagent was then used to determine the Fe(II) concentration in each sample. Original Fe(II) concentrations were calculated for Fe(III) reduction assays by accounting for dilutions and original Mn(IV) concentrations were calculated by accounting for the concentration of Fe(II) oxidized by Mn(IV) based on the following: Mn(IV) + 2Fe(II) = Mn(II) + 2Fe(III).

Homolog search and alignment

Homologs to each of the individual cytochrome conduit proteins were queried on 11-30-2016 in the Integrated Microbial Genomes database (Markowitz *et al.*, 2012) with a cutoff on 75% sequence length and 40% identity based on amino acid sequence within the Desulfuromonadales. A higher percent identity was demanded in this search due to the high

heme binding site density with the invariable CXXCH sequence. Only ExtJ and ExtL were excluded from the search and the OmcBC region was collapsed into a single cluster due to the high identity shared between the two copies. The gene neighborhood around each homolog hit was analyzed. With a few exceptions (see Table S2), all homologs were found to be conserved in gene clusters predicted to encode cytochrome conduits and containing several additional homologs to each corresponding *G. sulfurreducens* conduit. The proteins within each homologous cytochrome conduit that did not fall within the set cutoff were aligned to the amino acid sequence of the *G. sulfurreducens* component they replaced using ClustalΩ (Sievers *et al.*, 2011).

ACKNOWLEDGEMENTS

This research was supported by the Office of Naval Research (N000141210308). FJO is supported by the National Council of Science and Technology of Mexico (CONACYT).

AUTHOR CONTRIBUTIONS

FJO was responsible for the design of the study and the acquisition of data. Both FJO and DRB were responsible for the analysis and interpretation of the data; as well as writing of the manuscript.

ABBREVIATED SUMMARY

Geobacter sulfurreducens cells utilize electron conduits, or chains of redox proteins spanning the outer membrane, to transfer electrons to extracellular acceptors. Five different gene clusters encoding putative electron conduits were deleted in single- and multiple-gene-cluster markerless deletion strains. Mutants containing single conduit gene clusters each showed specific abilities to reduce Fe(III)- and Mn(IV)-oxides, Fe(III)-citrate and poised electrodes, and multiple conduits appeared to have overlapping roles during metal reduction. ExtABCD was the only electron conduit involved in electrode reduction.

REFERENCES

Aklujkar, M., Coppi, M.V., Leang, C., Kim, B.C., Chavan, M.A., Perpetua, L.A., *et al.* (2013) Proteins involved in electron transfer to Fe(III) and Mn(IV) oxides by *Geobacter sulfurreducens* and *Geobacter uraniireducens*. *Microbiology* **159**: 515–535.

Appel, J., Phunpruch, S., Steinmüller, K., and Schulz, R. (2000) The bidirectional hydrogenase of *Synechocystis sp.* PCC 6803 works as an electron valve during photosynthesis. *Arch Microbiol* **173**: 333–338.

Aussignargues, C., Giuliani, M.-C., Infossi, P., Lojou, E., Guiral, M., Giudici-Orticoni, M.-T., and Ilbert, M. (2012) Rhodanese functions as sulfur supplier for key enzymes in sulfur energy metabolism. *J Biol Chem* **287**: 19936–19948.

Bagos, P.G., Liakopoulos, T.D., Spyropoulos, I.C., and Hamodrakas, S.J. (2004) PRED-TMBB: a web server for predicting the topology of β-barrel outer membrane proteins. *Nucleic Acids Res* **32**: W400–W404.

Baron, D., LaBelle, E., Coursolle, D., Gralnick, J.A., and Bond, D.R. (2009) Electrochemical measurement of electron transfer kinetics by *Shewanella oneidensis* MR-1. *J Biol Chem* **284**: 28865–28873.

Bond, D.R., Holmes, D.E., Tender, L.M., and Lovley, D.R. (2002) Electrode-reducing microorganisms that harvest energy from marine sediments. *Science* **295**: 483–485.

Bond, D.R., and Lovley, D.R. (2003) Electricity production by *Geobacter sulfurreducens* attached to electrodes. *Appl Environ Microbiol* **69**: 1548–1555.

Chan, C.H., Levar, C.E., Otero, F.J., and Bond, D.R. (2017) Genome scale mutational analysis of *Geobacter sulfurreducens* reveals distinct molecular mechanisms for respiration and sensing of poised electrodes vs. Fe(III) oxides. *J Bacteriol* doi: 10.1128/JB.00340-17.

Chan, C.H., Levar, C.E., Zacharoff, L., Badalamenti, J.P., and Bond, D.R. (2015) Scarless genome editing and stable inducible expression vectors for *Geobacter sulfurreducens*. *Appl Environ Microbiol* **81**: 7178–7186.

Clarke, T.A., Edwards, M.J., Gates, A.J., Hall, A., White, G.F., Bradley, J., *et al.* (2011) Structure of a bacterial cell surface decaheme electron conduit. *Proc Natl Acad Sci* **108**: 9384–9389.

Coker, V.S., Byrne, J.M., Telling, N.D., Van Der Laan, G., Lloyd, J.R., Hitchcock, A.P., *et al.* (2012) Characterisation of the dissimilatory reduction of Fe(III)-oxyhydroxide at the microbe – mineral interface: the application of STXM–XMCD. *Geobiology* **10**: 347–354.

Coppi, M.V. (2005) The hydrogenases of *Geobacter sulfurreducens*: a comparative genomic perspective. *Microbiology* **151**: 1239–1254.

Coursolle, D., Baron, D.B., Bond, D.R., and Gralnick, J.A. (2010) The Mtr respiratory pathway is essential for reducing flavins and electrodes in *Shewanella oneidensis*. *J Bacteriol* **192**: 467–474.

603 Coursolle, D., and Gralnick, J.A. (2010) Modularity of the Mtr respiratory pathway of *Shewanella*
604 *oneidensis* strain MR-1. *Mol Microbiol* **77**: 995–1008.

605 Coursolle, D., and Gralnick, J.A. (2012) Reconstruction of extracellular respiratory pathways for
606 iron(III) reduction in *Shewanella oneidensis* strain MR-1. *Front Microbiol* **3**:56

607 Couture, R.-M., Charlet, L., Markelova, E., Madé, B., and Parsons, C.T. (2015) On–off
608 mobilization of contaminants in soils during redox oscillations. *Environ Sci Technol* **49**: 3015–
609 3023.

610 Cutting, R.S., Coker, V.S., Fellowes, J.W., Lloyd, J.R., and Vaughan, D.J. (2009) Mineralogical
611 and morphological constraints on the reduction of Fe(III) minerals by *Geobacter sulfurreducens*.
612 *Geochim Cosmochim Acta* **73**: 4004–4022.

613 Edwards, M.J., Hall, A., Shi, L., Fredrickson, J.K., Zachara, J.M., Butt, J.N., *et al.* (2012) The
614 crystal structure of the extracellular 11-heme cytochrome UndA reveals a conserved 10-heme
615 motif and defined binding site for soluble iron chelates. *Structure* **20**: 1275–1284.

616 Eusterhues, K., Hädrich, A., Neidhardt, J., Küsel, K., Keller, T.F., Jandt, K.D., and Totsche, K.U.
617 (2014) Reduction of ferrihydrite with adsorbed and coprecipitated organic matter: microbial
618 reduction by *Geobacter bremensis* vs. abiotic reduction by Na-dithionite. *Biogeosciences* **11**:
619 4953–4966.

620 Gennaris, A., Ezraty, B., Henry, C., Agrebi, R., Vergnes, A., Oheix, E., *et al.* (2015) Repairing
621 oxidized proteins in the bacterial envelope using respiratory chain electrons. *Nature* **528**: 409–
622 412.

623 Gralnick, J.A., and Newman, D.K. (2007) Extracellular respiration. *Mol Microbiol* **65**: 1–11.

624 Gralnick, J.A., Vali, H., Lies, D.P., and Newman, D.K. (2006) Extracellular respiration of
625 dimethyl sulfoxide by *Shewanella oneidensis* strain MR-1. *Proc Natl Acad Sci U S A* **103**: 4669–
626 4674.

627 Hartshorne, R.S., Reardon, C.L., Ross, D., Nuester, J., Clarke, T.A., Gates, A.J., *et al.* (2009)
628 Characterization of an electron conduit between bacteria and the extracellular environment.
629 *Proc Natl Acad Sci* **106**: 22169–22174.

630 Holmes, D.E., Bond, D.R., O'Neil, R.A., Reimers, C.E., Tender, L.R., and Lovley, D.R. (2004)
631 Microbial communities associated with electrodes harvesting electricity from a variety of aquatic
632 sediments. *Microb Ecol* **48**: 178–190.

633 Holmes, D.E., Chaudhuri, S.K., Nevin, K.P., Mehta, T., Methé, B.A., Liu, A., *et al.* (2006)
634 Microarray and genetic analysis of electron transfer to electrodes in *Geobacter sulfurreducens*.
635 *Environ Microbiol* **8**: 1805–1815.

636 Jiao, Y., and Newman, D.K. (2007) The *pio* operon is essential for phototrophic Fe(II) oxidation
637 in *Rhodopseudomonas palustris* TIE-1. *J Bacteriol* **189**: 1765–1773.

638 Juncker, A.S., Willenbrock, H., Heijne, G. von, Brunak, S., Nielsen, H., and Krogh, A. (2003)
639 Prediction of lipoprotein signal peptides in Gram-negative bacteria. *Protein Sci Publ Protein Soc*
640 **12**: 1652–1662.

641 Leang, C., Coppi, M.V., and Lovley, D.R. (2003) OmcB, a *c*-type polyheme cytochrome,
642 involved in Fe(III) reduction in *Geobacter sulfurreducens*. *J Bacteriol* **185**: 2096–2103.

643 Leang, C., and Lovley, D.R. (2005) Regulation of two highly similar genes, *omcB* and *omcC*, in
644 a 10 kb chromosomal duplication in *Geobacter sulfurreducens*. *Microbiology* **151**: 1761–1767.

645 Leang, C., Qian, X., Mester, T., and Lovley, D.R. (2010) Alignment of the *c*-type cytochrome
646 OmcS along pili of *Geobacter sulfurreducens*. *Appl Environ Microbiol* **76**: 4080–4084.

647 Levar, C.E., Chan, C.H., Mehta-Kolte, M.G., and Bond, D.R. (2014) An inner membrane
648 cytochrome required only for reduction of high redox potential extracellular electron acceptors.
649 *mBio* **5**: e02034-14.

650 Levar, C.E., Hoffman, C.L., Dunshee, A.J., Toner, B.M., and Bond, D.R. (2017) Redox potential
651 as a master variable controlling pathways of metal reduction by *Geobacter sulfurreducens*.
652 *ISME J* **11:** 741-752.

653 Liu, Y., Fredrickson, J.K., Zachara, J.M., and Shi, L. (2015) Direct involvement of *ombB*, *omaB*,
654 and *omcB* genes in extracellular reduction of Fe(III) by *Geobacter sulfurreducens* PCA.
655 *Microbiol Chem Geomicrobiol* 1075.

656 Liu, Y., Wang, Z., Liu, J., Levar, C., Edwards, M.J., Babauta, J.T., *et al.* (2014) A trans-outer
657 membrane porin-cytochrome protein complex for extracellular electron transfer by *Geobacter*
658 *sulfurreducens* PCA. *Environ Microbiol Rep* **6**: 776–785.

659 Logan, B.E., and Rabaey, K. (2012) Conversion of wastes into bioelectricity and chemicals by
660 using microbial electrochemical technologies. *Science* **337**: 686–690.

661 Majzlan, J. (2013) Minerals and aqueous species of iron and manganese as reactants and
662 products of microbial metal respiration. In *Microbial Metal Respiration*. Gescher, J., and Kappler,
663 A. (eds). Springer Berlin Heidelberg, pp. 1–28

664 Markowitz, V.M., Chen, I.-M.A., Palaniappan, K., Chu, K., Szeto, E., Grechkin, Y., *et al.* (2012)
665 IMG: the integrated microbial genomes database and comparative analysis system. *Nucleic*
666 *Acids Res* **40**: D115–D122.

667 Marsili, E., Sun, J., and Bond, D.R. (2010) Voltammetry and growth physiology of *Geobacter*
668 *sulfurreducens* biofilms as a function of growth stage and imposed electrode potential.
669 *Electroanalysis* **22**: 865–874.

670 Methé, B.A., Nelson, K.E., Eisen, J.A., Paulsen, I.T., Nelson, W., Heidelberg, J.F., *et al.* (2003)
671 Genome of *Geobacter sulfurreducens*: Metal reduction in subsurface environments. *Science*
672 **302**: 1967–1969.

673 Navrotsky, A., Mazeina, L., and Majzlan, J. (2008) Size-driven structural and thermodynamic
674 complexity in iron oxides. *Science* **319**: 1635–1638.

675 Nelson, C.E., Rogowski, A., Morland, C., Wilhide, J.A., Gilbert, H.J., and Gardner, J.G. (2017)
676 Systems analysis in *Cellvibrio japonicus* resolves predicted redundancy of β-glucosidases and
677 determines essential physiological functions. *Mol Microbiol* **104**;2 294.

678 Nevin, K.P., Kim, B.-C., Glaven, R.H., Johnson, J.P., Woodard, T.L., Methé, B.A., *et al.* (2009)
679 Anode biofilm transcriptomics reveals outer surface components essential for high density
680 current production in *Geobacter sulfurreducens* fuel cells. *PLOS ONE* **4**: e5628.

681 N'Guessan, A.L., Vrionis, H.A., Resch, C.T., Long, P.E., and Lovley, D.R. (2008) Sustained
682 removal of uranium from contaminated groundwater following stimulation of dissimilatory metal
683 reduction. *Environ Sci Technol* **42**: 2999–3004.

684 Peng, L., and Zhang, Y. (2017) Cytochrome OmcZ is essential for the current generation by
685 *Geobacter sulfurreducens* under low electrode potential. *Electrochimica Acta* **228**: 447–452.

686 Prat, L., Maillard, J., Rohrbach-Brandt, E., and Holliger, C. (2012) An unusual tandem-domain
687 rhodanese harbouring two active sites identified in *Desulfitobacterium hafniense*. *FEBS J* **279**:
688 2754–2767.

689 Qian, X., Mester, T., Morgado, L., Arakawa, T., Sharma, M.L., Inoue, K., *et al.* (2011)
690 Biochemical characterization of purified OmcS, a *c*-type cytochrome required for insoluble
691 Fe(III) reduction in *Geobacter sulfurreducens*. *Biochim Biophys Acta BBA - Bioenerg* **1807**:
692 404–412.

693 Qiu, Y., Cho, B.-K., Park, Y.S., Lovley, D., Palsson, B.Ø., and Zengler, K. (2010) Structural and
694 operational complexity of the *Geobacter sulfurreducens* genome. *Genome Res* **20**: 1304–1311.

695 Ramírez, P., Toledo, H., Guiliani, N., and Jerez, C.A. (2002) An exported rhodanese-like protein
696 is induced during growth of *Acidithiobacillus ferrooxidans* in metal sulfides and different sulfur
697 compounds. *Appl Environ Microbiol* **68**: 1837–1845.

698 Ravot, G., Casalot, L., Ollivier, B., Loison, G., and Magot, M. (2005) *rdlA*, a new gene encoding
699 a rhodanese-like protein in *Halanaerobium congolense* and other thiosulfate-reducing
700 anaerobes. *Res Microbiol* **156**: 1031–1038.

701 Ren, Z., Steinberg, L.M., and Regan, J.M. (2008) Electricity production and microbial biofilm
702 characterization in cellulose-fed microbial fuel cells. *Water Sci Technol* **58**: 617–622.

703 Richardson, D.J., Butt, J.N., Fredrickson, J.K., Zachara, J.M., Shi, L., Edwards, M.J., *et al.*
704 (2012) The "porin–cytochrome" model for microbe-to-mineral electron transfer. *Mol Microbiol* **85**:
705 201–212.

706 Richter, H., P. Nevin, K., Jia, H., A. Lowy, D., R. Lovley, D., and M. Tender, L. (2009) Cyclic
707 voltammetry of biofilms of wild type and mutant *Geobacter sulfurreducens* on fuel cell anodes
708 indicates possible roles of OmcB, OmcZ, type IV pili, and protons in extracellular electron
709 transfer. *Energy Environ Sci* **2**: 506–516.

710 Robuschi, L., Tomba, J.P., Schrott, G.D., Bonanni, P.S., Desimone, P.M., and Busalmen, J.P.
711 (2013) Spectroscopic slicing to reveal internal redox gradients in electricity-producing biofilms.
712 *Angew Chem Int Ed* **52**: 925–928.

713 Schievano, A., Pepé Sciarria, T., Vanbroekhoven, K., De Wever, H., Puig, S., Andersen, S.J., *et*
714 *al.* (2016) Electro-fermentation – Merging electrochemistry with fermentation in industrial
715 applications. *Trends Biotechnol* **34**:11 866-878.

716 Schrader, P.S., Reimers, C.E., Girguis, P., Delaney, J., Doolan, C., Wolf, M., and Green, D.
717 (2016) Independent benthic microbial fuel cells powering sensors and acoustic communications
718 with the MARS underwater observatory. *J Atmospheric Ocean Technol* **33**: 607–617.

719 Shelobolina, E.S., Coppi, M.V., Korenevsky, A.A., DiDonato, L.N., Sullivan, S.A., Konishi, H., *et*
720 *al.* (2007) Importance of *c*-type cytochromes for U(VI) reduction by *Geobacter sulfurreducens*.
721 *BMC Microbiol* **7**: 16.

722 Shi, L., Dong, H., Reguera, G., Beyenal, H., Lu, A., Liu, J., *et al.* (2016) Extracellular electron
723 transfer mechanisms between microorganisms and minerals. *Nat Rev Microbiol* **14**: 651–662.

724 Sievers, F., Wilm, A., Dineen, D., Gibson, T.J., Karplus, K., Li, W., *et al.* (2011) Fast, scalable
725 generation of high-quality protein multiple sequence alignments using Clustal Omega. *Mol Syst*
726 *Biol Mol Syst Biol* **7**, **7**: 539, 539–539.

727 Simon, R., Priefer, U., and Pühler, A. (1983) A broad host range mobilization system for in vivo
728 genetic engineering: Transposon mutagenesis in Gram negative bacteria. *Nat Biotechnol* **1**:
729 784–791.

730 Smith, J.A., Tremblay, P.-L., Shrestha, P.M., Snoeyenbos-West, O.L., Franks, A.E., Nevin, K.P.,
731 and Lovley, D.R. (2014) Going wireless: Fe(III) oxide reduction without pili by *Geobacter*
732 *sulfurreducens* strain JS-1. *Appl Environ Microbiol* **80**: 4331–4340.

733 Snider, R.M., Strycharz-Glaven, S.M., Tsoi, S.D., Erickson, J.S., and Tender, L.M. (2012) Long-
734 range electron transport in *Geobacter sulfurreducens* biofilms is redox gradient-driven. *Proc Natl*
735 *Acad Sci* **109**: 15467–15472.

736 Stephen, C.S., LaBelle, E.V., Brantley, S.L., and Bond, D.R. (2014) Abundance of the
737 multiheme *c*-type cytochrome OmcB increases in outer biofilm layers of electrode-grown
738 *Geobacter sulfurreducens*. *PLOS ONE* **9**: e104336.

739 Tadanier, C.J., Schreiber, M.E., and Roller, J.W. (2005) Arsenic mobilization through microbially
740 mediated deflocculation of ferrihydrite. *Environ Sci Technol* **39**: 3061–3068.

741 Toner, B.M., Fakra, S.C., Manganini, S.J., Santelli, C.M., Marcus, M.A., Moffett, J.W., *et al.*
742 (2009) Preservation of iron(II) by carbon-rich matrices in a hydrothermal plume. *Nat Geosci* **2**:
743 197–201.

744 Tremblay, P.-L., Summers, Z.M., Glaven, R.H., Nevin, K.P., Zengler, K., Barrett, C.L., *et al.*
745 (2011) A *c*-type cytochrome and a transcriptional regulator responsible for enhanced
746 extracellular electron transfer in *Geobacter sulfurreducens* revealed by adaptive evolution.
747 *Environ Microbiol* **13**: 13–23.

748 Ueki, T., DiDonato, L.N., and Lovley, D.R. (2017) Toward establishing minimum requirements
749 for extracellular electron transfer in *Geobacter sulfurreducens*. *FEMS Microbiol Lett* **364:**9

Wang, Z., Liu, C., Wang, X., Marshall, M.J., Zachara, J.M., Rosso, K.M., *et al.* (2008) Kinetics of reduction of Fe(III) complexes by outer membrane cytochromes MtrC and OmcA of *Shewanella oneidensis* MR-1. *Appl Environ Microbiol* **74**: 6746–6755.

White, G.F., Shi, Z., Shi, L., Wang, Z., Dohnalkova, A.C., Marshall, M.J., *et al.* (2013) Rapid electron exchange between surface-exposed bacterial cytochromes and Fe(III) minerals. *Proc Natl Acad Sci* **110**: 6346–6351.

Williams, K.H., Long, P.E., Davis, J.A., Wilkins, M.J., N'Guessan, A.L., Steefel, C.I., *et al.* (2011) Acetate availability and its influence on sustainable bioremediation of uranium-contaminated groundwater. *Geomicrobiol J* **28**: 519–539.

Yelton, A.P., Williams, K.H., Fournelle, J., Wrighton, K.C., Handley, K.M., and Banfield, J.F. (2013) Vanadate and acetate biostimulation of contaminated sediments decreases diversity, selects for specific taxa, and decreases aqueous V5+ soncentration. *Environ Sci Technol* **47**: 6500–6509.

Yu, N.Y., Wagner, J.R., Laird, M.R., Melli, G., Rey, S., Lo, R., *et al.* (2010) PSORTb 3.0: improved protein subcellular localization prediction with refined localization subcategories and predictive capabilities for all prokaryotes. *Bioinformatics* **26**: 1608–1615.

Zacharoff, L., Chan, C.H., and Bond, D.R. (2016) Reduction of low potential electron acceptors requires the CbcL inner membrane cytochrome of *Geobacter sulfurreducens*. *Bioelectrochemistry* **107**: 7–13.

771 **Tables**:

772

773 **Table 1**

Strains and Plasmids	Description or relevant genotype	Reference
Geobacter sulfurreducens strains		
DB1279	ΔGSU2731-39 (Δ*omcBC*)	Chan *et al*., 2017
DB1280	ΔGSU2645-42 (Δ*extABCD*)	Chan *et al*., 2017
DB1281	ΔGSU2940-36 (Δ*extHIJKL*)	Chan *et al*., 2017
DB1282	ΔGSU2724-26 (Δ*extEFG*)	Chan *et al*., 2017
DB1487	ΔGSU2731-39 ΔGSU2645-42 (Δ*omcBC* Δ*extABCD*)	This study
DB1488	ΔGSU2731-39 ΔGSU2724-26 (Δ*omcBC* Δ*extEFG*)	This study
DB1289	ΔGSU2731-39 ΔGSU2940-36 (Δ*omcBC* Δ*extHIJKL*)	This study
DB1489	ΔGSU2645-42 ΔGSU2724-26 (Δ*extABCD* Δ*extEFG*)	This study
DB1490	ΔGSU2645-42 ΔGSU2940-36 (Δ*extABCD* Δ*extHIJKL*)	This study
DB1290	ΔGSU2731-39 ΔGSU2940-36 ΔGSU2724-26 (*extA*$^{+}$)	This study
DB1291	ΔGSU2731-39 ΔGSU2645-42 ΔGSU2936-2940 (*extEFG*$^{+}$)	This study
DB1491	ΔGSU2731-39 ΔGSU2645-42 ΔGSU2726-24 (*extHIJKL*$^{+}$)	This study
DB1492	ΔGSU2645-42 ΔGSU2726-24 Δ2940-36 (*omcBC*$^{+}$)	This study
DB1493	ΔGSU2731-39 ΔGSU2645-42 ΔGSU2726-24 ΔGSU2940-36 (Δ5)	This study
Escherichia coli strains		
S17-1	*recA pro hsdR* RP4-2-Tc::Mu-Km::Tn7	Simon *et al*., 1983
Plasmids		
pK18*mobsacB*		Simon *et al*., 1983
pRK2-Geo2		Chan *et al*., 2015
p*DomcBC*	Flanking regions of *omcBC* in pK18*mobsacB*	This study
p*DextABCD*	Flanking regions of *extABCD* in pK18*mobsacB*	This study
p*DextEFG*	Flanking regions of *extEFG* in pK18*mobsacB*	This study
p*DextHIJKL*	Flanking regions of *extHIJKL* in pK18*mobsacB*	This study
p*omcB*	*ombB-omaB-omcB* in pRK2-Geo2	This study
p*extABCD*	*extABCD* in pRK2-Geo2	This study

774

775

776

777 **Table 1. Strains and plasmids used in this study.**

Table 2

	% of wild type								
Substrate	Δ*omcBC*	Δ*extABCD*	Δ*extEFG*	Δ*extHIJKL*	*omcBC*$^+$	*extABCD*$^+$	*extEFG*$^+$	*extHIJKL*$^+$	Δ5
Fe(III)-citrate	61.2	105	62.5	66.3	101.1	99.2	22.5	23.8	0.1
Fe(III)-oxide	68.9	83.3	87.5	95.8	78.8	29.2	60.4	52.1	0.1
Mn(IV)-oxide	94.5	95.1	99.6	97.9	83.3	26.7	86.8	75.6	1.7
Electrode	76.5	20.9	104.8	86.3	28.3	137.9	21.2	25.9	21.9

Table 2. Performance of *G. sulfurreducens* strains lacking one cluster, or containing only one cluster. Growth of single cytochrome conduit deletion mutants and mutants lacking all except one cytochrome conduit, averaged from all incubations and represented as the percent of wild type growth. Averages calculated from n ≥ 8 experiments.

Figure Legends

Figure 1. The outer membrane electron conduit gene clusters of *G. sulfurreducens*. A) Genetic organization and predicted features of operons containing putative outer membrane conduits. Deletion constructs indicated by dashed line. B) Identity matrix from amino acid sequence alignment of each cytochrome or ß-barrel component using ClustalΩ.

Figure 2. Only ExtABCD conduit is involved in electrode reduction. Current density produced by A) single and B) multiple-cluster deletion mutants on graphite electrodes poised at +0.24 V vs. SHE. All mutants were grown in at least two separate experiments, and curves are representative of n ≥ 3 independent replicates. Similar results were obtained at lower (-0.1 V vs. SHE) redox potentials.

Figure 3. Effect of kanamycin on final current density, and comparison of ExtABCD and OmcBC complementation. A) Final current density of wild type *G. sulfurreducens* compared to wild type carrying an empty vector in the presence of increasing kanamycin concentrations. B) Current density produced by Δ5 strain plus either *extABCD* or *omcB* cluster-containing vectors, in the presence of 5 µg/ml residual kanamycin. Wild type and Δ5 strains carrying the empty vector were used as controls. All experiments were conducted in duplicate and curves are representative of n ≥ 3 replicates.

Figure 4. No single outer membrane cluster is essential but all are functional for electron transfer to Fe(III)- and Mn(IV)-oxides. Growth of single cluster deletion mutants and triple mutants lacking all but one cytochrome conduit, as well as Δ5 mutant lacking all clusters utilizing A) 70 mM Fe(III)-oxide or B) 20 mM Mn(IV)-oxide as terminal electron acceptor. All experiments were conducted in triplicate and curves are average ± SD of n ≥ 3 replicates.

Figure 5. OmcBC and ExtEFG have dominant roles in Fe(III) and Mn(IV) oxide reduction. Reduction of A) 70 mM Fe(III)-oxide or B) 20 mM Mn(IV)-oxide by the Δ*omcBC* strain and additional deletions in an Δ*omcBC* background. All experiments were conducted in triplicate and curves are average ± SD of n ≥ 3 replicates.

Figure 6. Co-presence of multiple conduit complexes is responsible for wild-type levels of metal oxide reduction. Reduction of A) 70 mM Fe(III)-oxide or B) 20 mM Mn(IV)-oxide by the Δ5 mutant expressing *extABCD* or the *omcB* cluster compared to the empty vector control. All experiments were conducted in triplicate and curves are average ± SD of n ≥ 3 replicates.

Figure 7. OmcBC and ExtABCD are the key cytochromes during Fe(III)-citrate reduction. Growth using 55 mM Fe(III)-citrate as an electron acceptor by A) single conduit cluster deletion

mutants, B) triple mutants lacking all but one cytochrome conduit, as well as the Δ5 strain lacking all five cytochrome conduits, C) mutants in an Δ*omcBC* background strain, and D) Δ5 mutants expressing *omcB* or *extABCD* or carrying an empty expression vector as control. All experiments were conducted in triplicate and curves are average ± SD of n ≥ 3 replicates.

Figure 8. Cytochrome conduit conservation across the Order Desulfuromonodales. Schematic representation of cytochrome conduits from the Desulfuromonodales with homologs to either A) OmcBC, B) ExtABCD, C) ExtEFG, or D) ExtHIJKL. Red arrows = putative outer membrane products with a predicted lipid attachment site, yellow arrows = predicted periplasmic components, and green arrows = predicted outer membrane anchor components. Complete clusters with all components sharing >40% identity to the corresponding *G. sulfurreducens* cytochrome conduit are represented in boxes to the left of each gene cluster. Clusters in which one or more proteins are replaced by a new element with <40% identity are listed on the right side of each gene cluster. Proteins with numbers indicate the % identity to the *G. sulfurreducens* version. [a]OmcBC homologs in these gene clusters also encoding Hox hydrogenase complexes. [b]Gene clusters have contiguous *extBCD* loci but *extA* is not in near vicinity, as *extA* were found un-clustered in separate parts of the genome for some of those organisms (see Supplemental Table S2). [c]Gene cluster has additional lipoprotein decaheme *c*-cytochrome upstream of *extE*. [d]Lipid attachment sites corresponding to ExtJL could not be found but there is an additional small lipoprotein encoded within the gene cluster. For ExtHIJKL encoding clusters, homologs depicted above *extH* are found in gene clusters containing only *extI*, whereas homologs depicted below *extH* are found in gene clusters containing full *extHIJKL* loci. Upstream and on the opposite strand to all gene clusters homologous to *extHIJKL* there is a transcription regulator of the LysR family, except [e], where there is no transcriptional regulator in that region, and [f], where there are transcriptional regulators of the TetR family instead.

Figure 1.

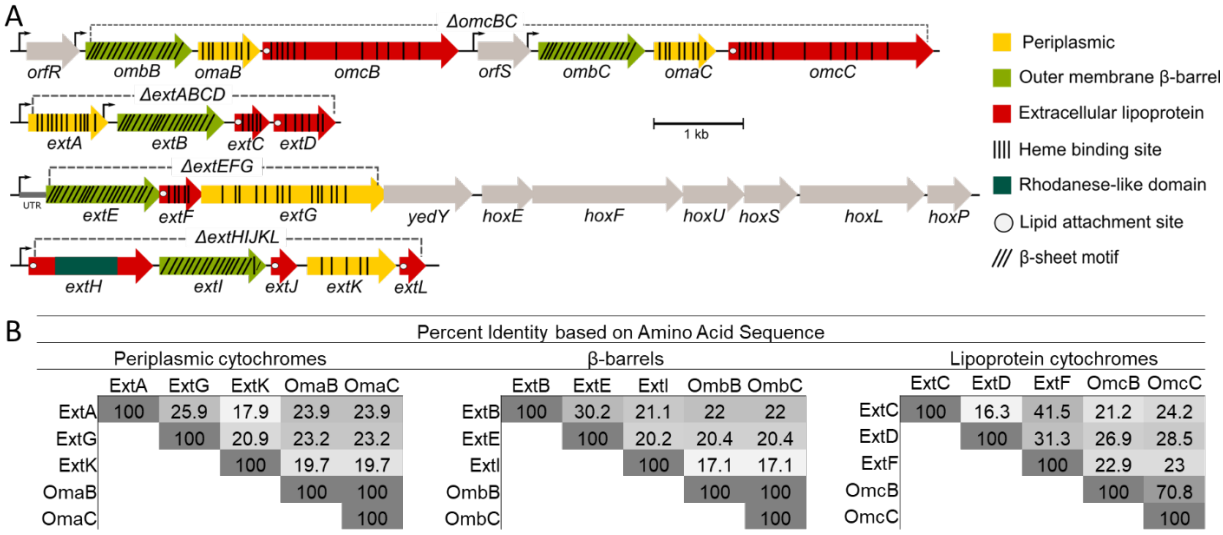

B

Percent Identity based on Amino Acid Sequence

Periplasmic cytochromes

	ExtA	ExtG	ExtK	OmaB	OmaC
ExtA	100	25.9	17.9	23.9	23.9
ExtG		100	20.9	23.2	23.2
ExtK			100	19.7	19.7
OmaB				100	100
OmaC					100

β-barrels

	ExtB	ExtE	ExtI	OmbB	OmbC
ExtB	100	30.2	21.1	22	22
ExtE		100	20.2	20.4	20.4
ExtI			100	17.1	17.1
OmbB				100	100
OmbC					100

Lipoprotein cytochromes

	ExtC	ExtD	ExtF	OmcB	OmcC
ExtC	100	16.3	41.5	21.2	24.2
ExtD		100	31.3	26.9	28.5
ExtF			100	22.9	23
OmcB				100	70.8
OmcC					100

Figure 1. The outer membrane electron conduit gene clusters of *G. sulfurreducens*. A) Genetic organization and predicted features of operons containing putative outer membrane conduits. Deletion constructs indicated by dashed line. B) Identity matrix from amino acid sequence alignment of each cytochrome or ß-barrel component using ClustalΩ.

Figure 2.

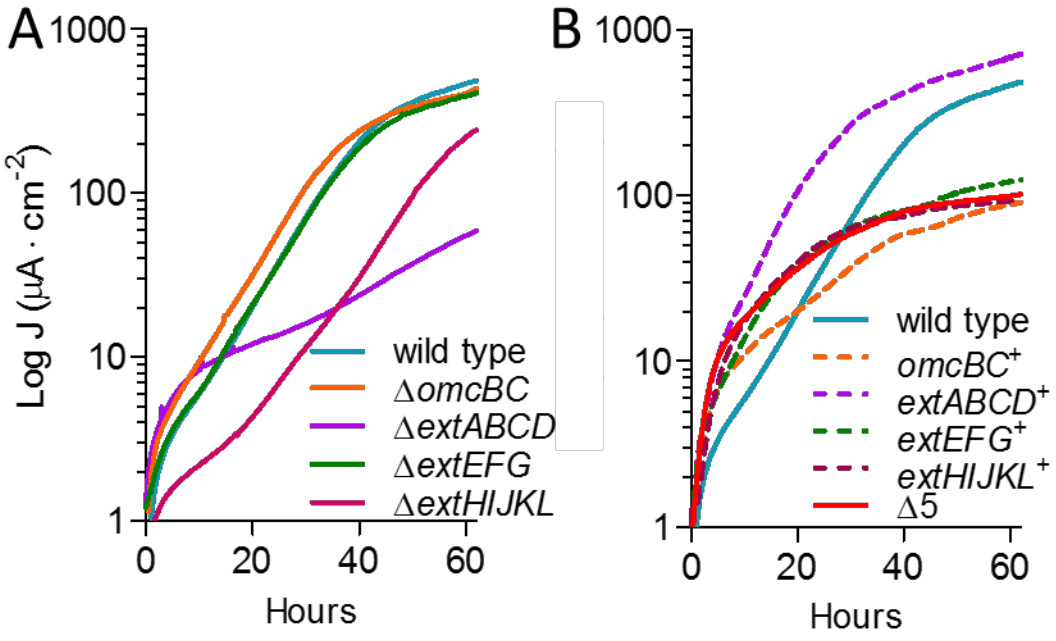

Figure 2. Only ExtABCD conduit is involved in electrode reduction. Current density produced by A) single and B) multiple-cluster deletion mutants on graphite electrodes poised at +0.24 V vs. SHE. All mutants were grown in at least two separate experiments, and curves are representative of n ≥ 3 independent replicates. Similar results were obtained at lower (-0.1 V vs. SHE) redox potentials.

Figure 3.

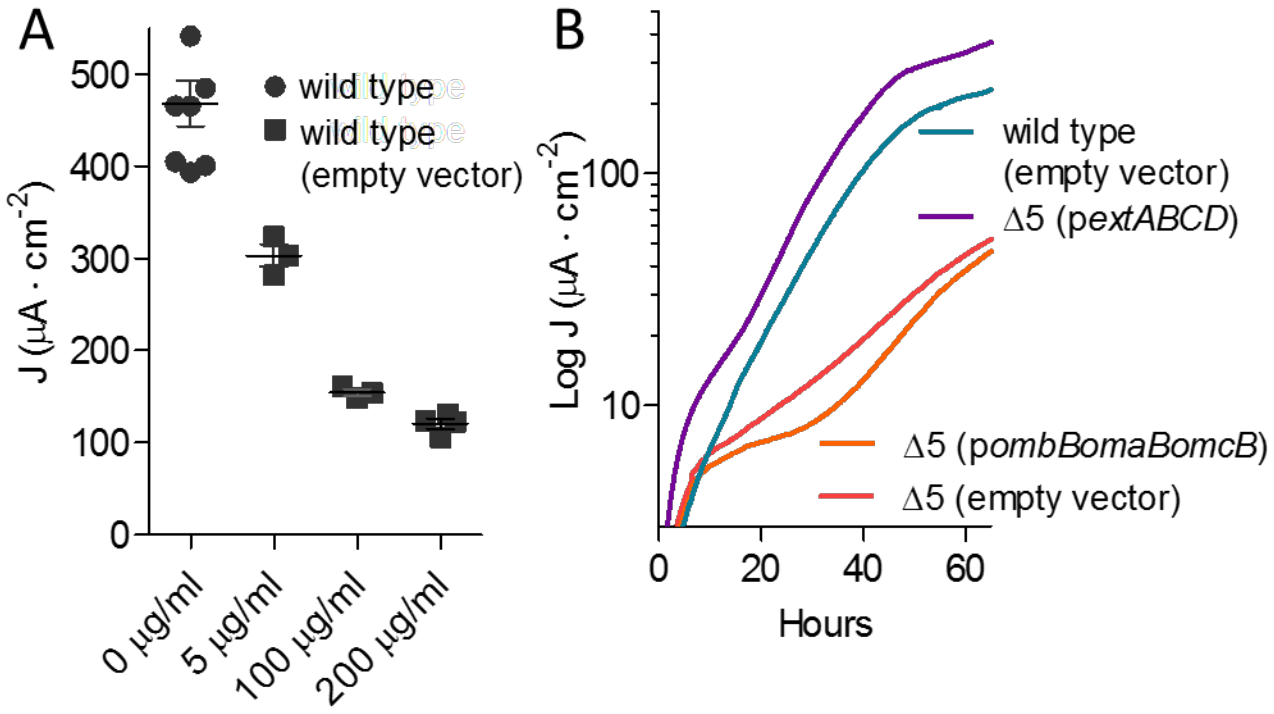

Figure 3. Effect of kanamycin on final current density, and comparison of ExtABCD and OmcBC complementation. A) Final current density of wild type *G. sulfurreducens* compared to wild type carrying an empty vector in the presence of increasing kanamycin concentrations. B) Current density produced by Δ5 strain plus either *extABCD* or *omcB* cluster-containing vectors, in the presence of 5 μg/ml residual kanamycin. Wild type and Δ5 strains carrying the empty vector were used as controls. All experiments were conducted in duplicate and curves are representative of n ≥ 3 replicates.

Figure 4.

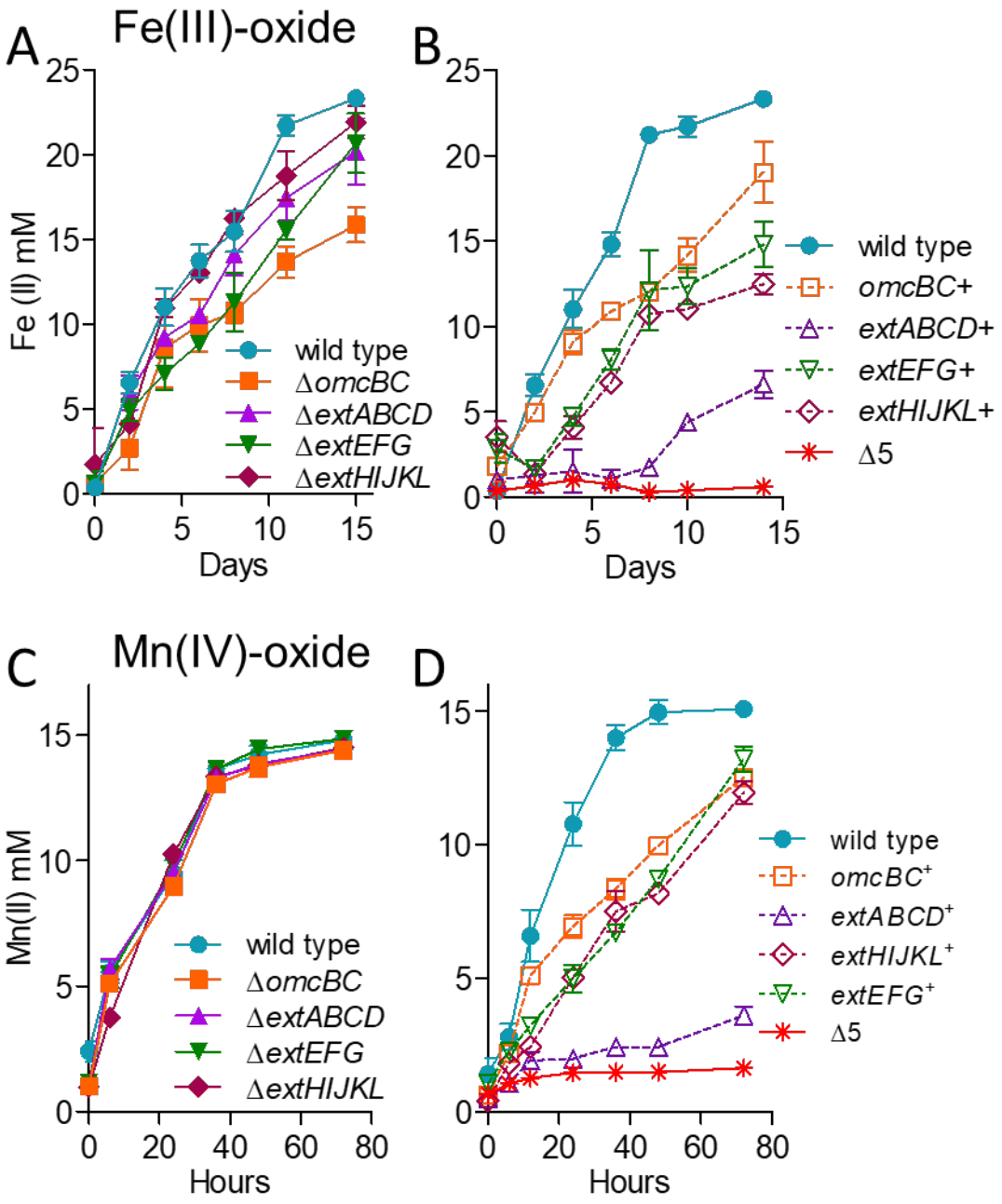

Figure 4. No single outer membrane cluster is essential but all are functional for electron transfer to Fe(III)- and Mn(IV)-oxides. Growth of single cluster deletion mutants and triple mutants lacking all but one cytochrome conduit, as well as Δ5 mutant lacking all clusters utilizing A) 70 mM Fe(III)-oxide or B) 20 mM Mn(IV)-oxide as terminal electron acceptor. All experiments were conducted in triplicate and curves are average ± SD of n ≥ 3 replicates.

Figure 5.

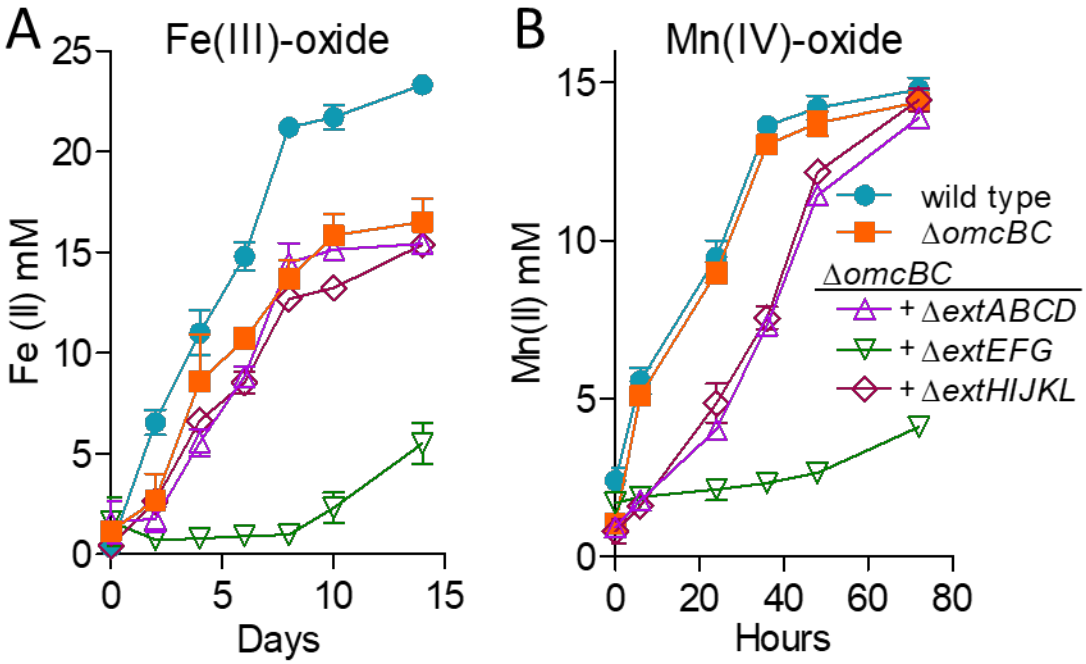

Figure 5. OmcBC and ExtEFG have dominant roles in Fe(III) and Mn(IV) oxide reduction. Reduction of A) 70 mM Fe(III)-oxide or B) 20 mM Mn(IV)-oxide by the Δ*omcBC* strain and additional deletions in an Δ*omcBC* background. All experiments were conducted in triplicate and curves are average ± SD of n ≥ 3 replicates.

Figure 6.

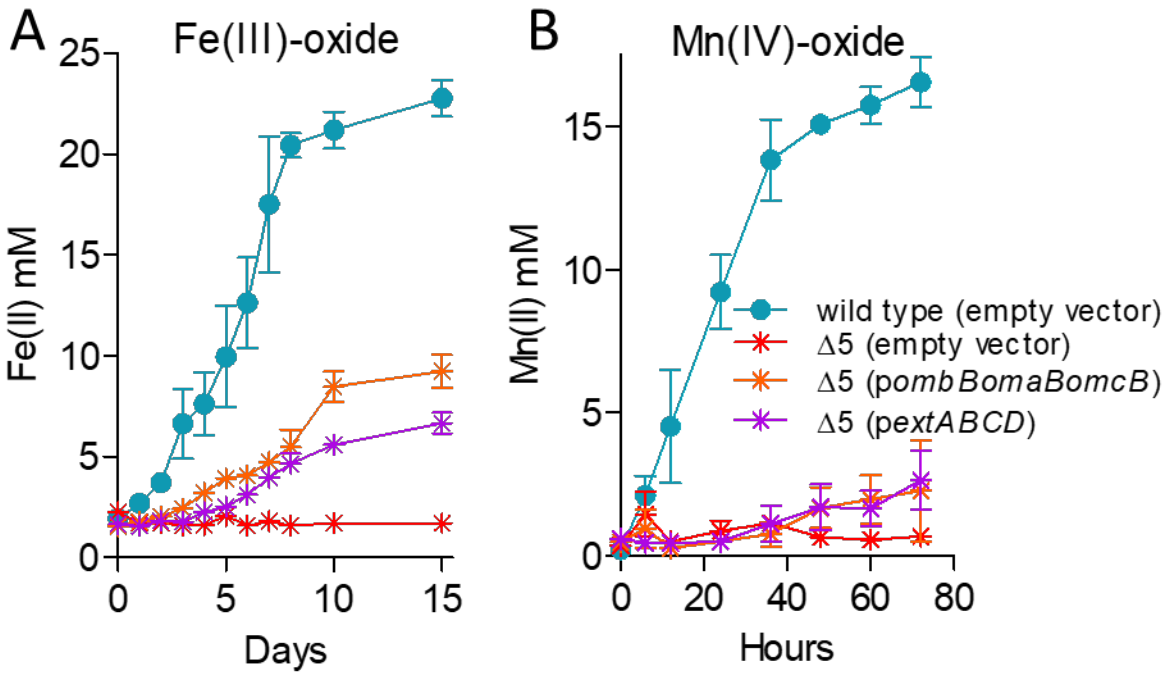

Figure 6. Co-presence of multiple conduit complexes is responsible for wild-type levels of metal oxide reduction. Reduction of A) 70 mM Fe(III)-oxide or B) 20 mM Mn(IV)-oxide by the Δ5 mutant expressing *extABCD* or the *omcB* cluster compared to the empty vector control. All experiments were conducted in triplicate and curves are average ± SD of n ≥ 3 replicates.

Figure 7.

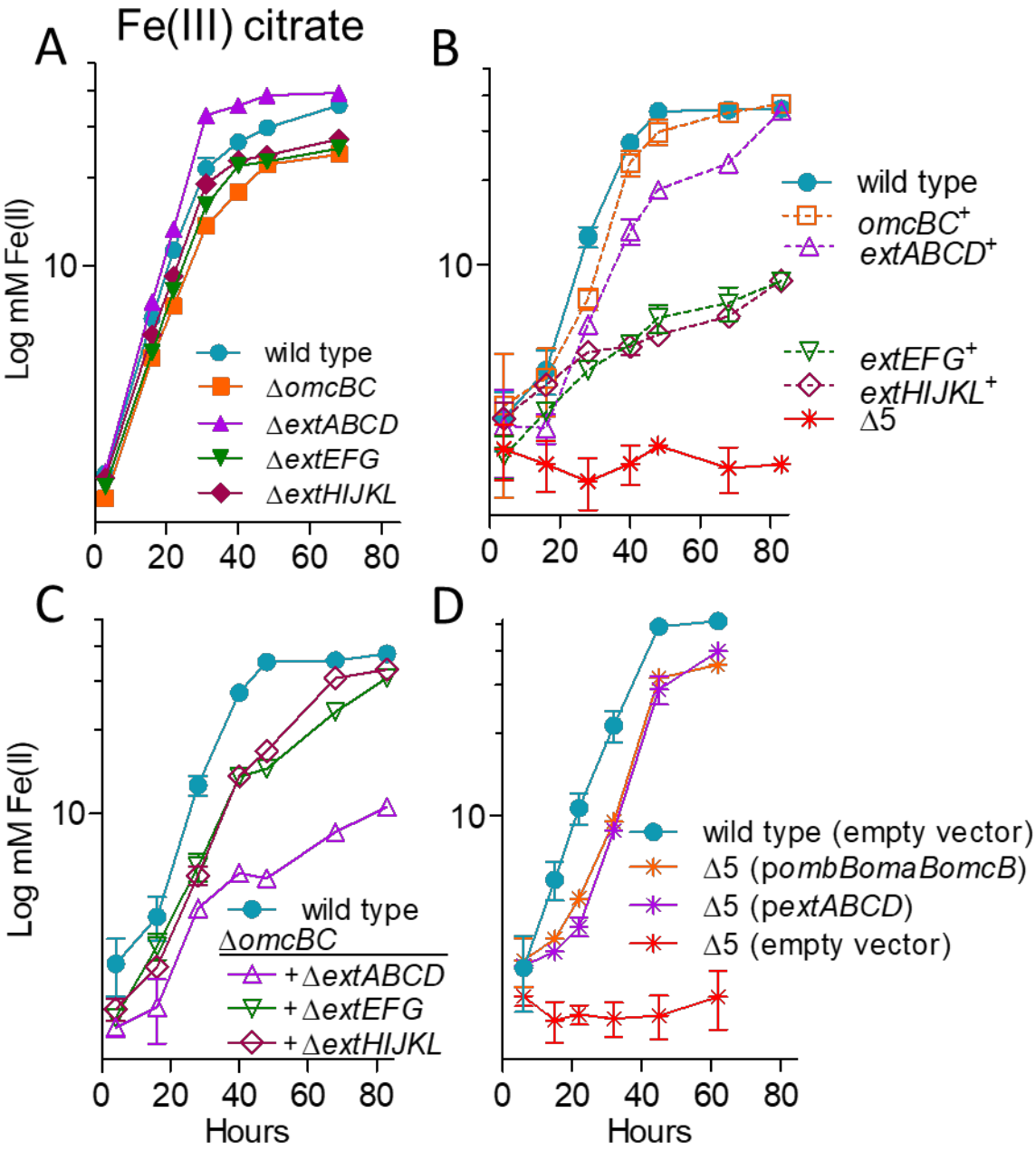

Figure 7. OmcBC and ExtABCD are the key cytochromes during Fe(III)-citrate reduction. Growth using 55 mM Fe(III)-citrate as an electron acceptor by A) single conduit cluster deletion mutants, B) triple mutants lacking all but one cytochrome conduit, as well as the Δ5 strain lacking all five cytochrome conduits, C) mutants in an Δ*omcBC* background strain, and D) Δ5 mutants expressing *omcB* or *extABCD* or carrying an empty expression vector as control. All experiments were conducted in triplicate and curves are average ± SD of n ≥ 3 replicates.

Figure 8.

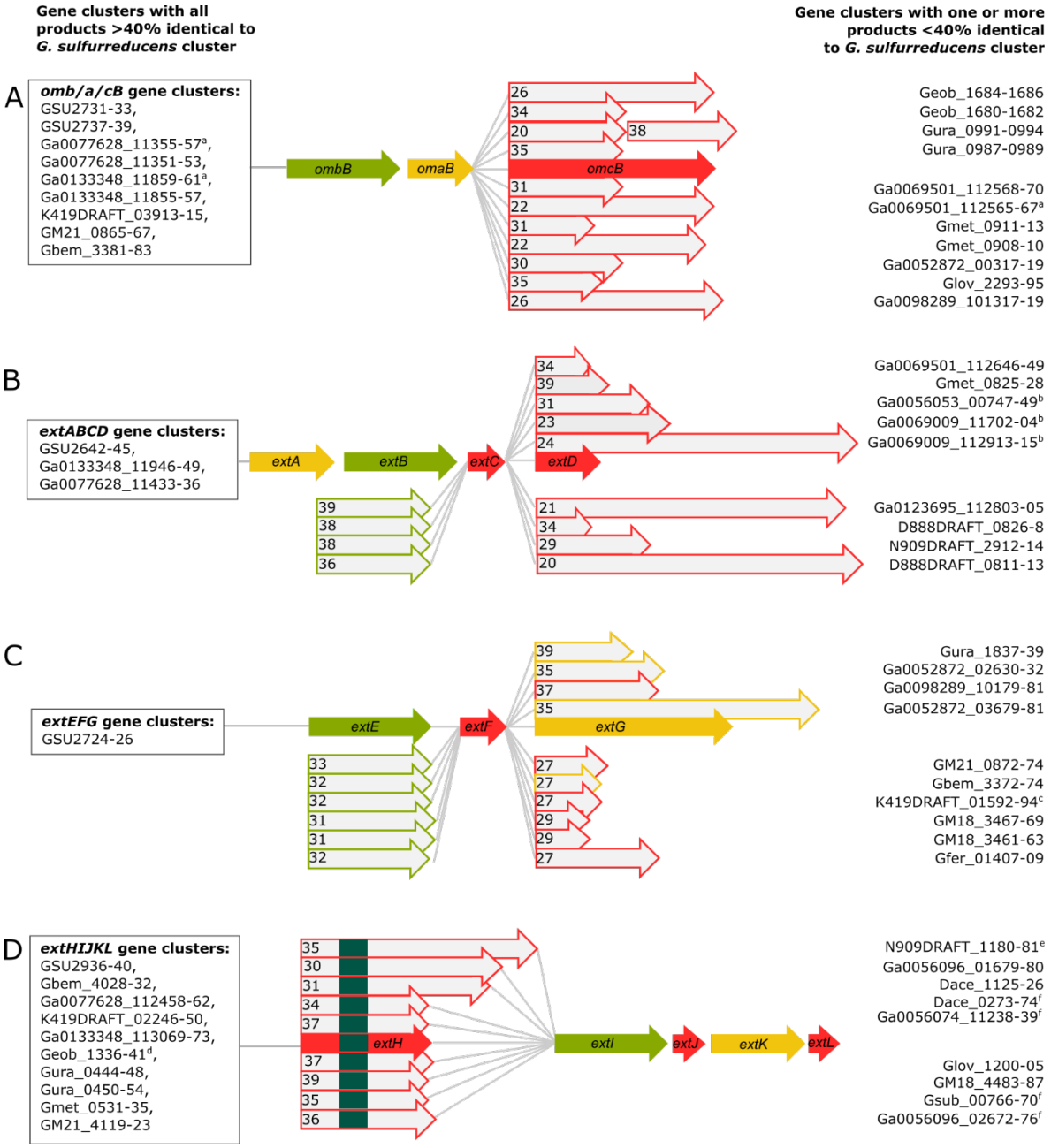

Figure 8. Cytochrome conduit conservation across the Order Desulfuromonodales. Schematic representation of cytochrome conduits from the Desulfuromonodales with homologs to either A) OmcBC, B) ExtABCD, C) ExtEFG, or D) ExtHIJKL. Red arrows = putative outer membrane products with a predicted lipid attachment site, yellow arrows = predicted periplasmic components, and green arrows = predicted outer membrane anchor components. Complete clusters with all components sharing >40% identity to the corresponding *G. sulfurreducens* cytochrome conduit are represented in boxes to the left of each gene cluster. Clusters in which

one or more proteins are replaced by a new element with <40% identity are listed on the right side of each gene cluster. Proteins with numbers indicate the % identity to the *G. sulfurreducens* version. [a]OmcBC homologs in these gene clusters also encoding Hox hydrogenase complexes. [b]Gene clusters have contiguous *extBCD* loci but *extA* is not in near vicinity, as *extA* were found un-clustered in separate parts of the genome for some of those organisms (see Supplemental Table S2). [c]Gene cluster has additional lipoprotein decaheme *c*-cytochrome upstream of *extE*. [d]Lipid attachment sites corresponding to ExtJL could not be found but there is an additional small lipoprotein encoded within the gene cluster. For ExtHIJKL encoding clusters, homologs depicted above *extH* are found in gene clusters containing only *extI*, whereas homologs depicted below *extH* are found in gene clusters containing full *extHIJKL* loci. Upstream and on the opposite strand to all gene clusters homologous to *extHIJKL* there is a transcription regulator of the LysR family, except [e], where there is no transcriptional regulator in that region, and [f], where there are transcriptional regulators of the TetR family instead.